Sensors & Transducers, Vol. 230, Issue 2, February 2019, pp. 31-38

www.sensorsportal.com

Sensors & Transducers

Published by IFSA Publishing, S. L., 2019
http://www.sensorsportal.com

Comparative Studies of Hybrid Model-Dependent and Model-Free Controller Application on Crane System

[1] Haliru LIMAN, [2, *] Nura Musa TAHIR, [2] Godwin SANI, [1] Ejike Chibuzo ANENE and [2] Adamu Yawale BABAWURO

[1] Department of Electrical Engineering,
Abubakar Tafawa Balewa University (ATBU) Bauchi, Nigeria
[2] Department of Mechatronics and System Engineering,
Abubakar Tafawa Balewa University (ATBU) Bauchi, Nigeria
E-mail: nuratahir85@gmail.com, mtnura@atbu.edu.ng

Received: 20 January 2019 /Accepted: 20 February 2019 /Published: 28 February 2019

Abstract: Gantry Crane is a machine used for shipping of goods from one point to another. Speed, accuracy and safety are of paramount importance in gantry crane (GC) operation, but operating GC results in unwanted sway which degrades the accuracy and safety. In this paper, hybrid control schemes are proposed for precise trolley position control and sway suppression in GC systems. Output Based input shaping (OBIS) filter was designed using the output of the system for sway suppression and proportional integral derivative (PID), linear quadratic regulator (LQR), higher order differential feedback (HODF) controllers were incorporated separately for precise trolley position control. Based on the analysis of the Simulation results, it was observed that LQR-OBIS controller shown more precise tracking and higher sway reduction control. But HODFC-OBIS is a model-free control schemes hence more robust.

Keywords: Gantry crane, OBIS filter, LQR, Sway, HODFC, Model-free.

1. Introduction

Cranes are flexible mechanical systems usually employed for loading and unloading heavy objects in industries and civil construction sites. Ensuring minimum payload sway is significant in achieving efficient production rate which at the same time needs faster system directional technique [1]. Payload hoisting is regarded as an essential aspect of crane directional feature which in general leads to undesirable crane motions such as bouncing, swinging and twisting. These crane motions have devastating effects on the system overall efficiency, operation safety and payload positioning [2]. Feedback and feedforward sway control techniques were reported to have been applied in flexible systems.

The feedforward approach is employed for the alteration of input signals for sway cancellation while the crane system's states estimation as well as reduction of oscillation effects on payload positioning is achieved by feedback control technique. Hence, better system performance in terms of free-vibration is obtained by combining the two sway control techniques. The feedforward strategy contributes in minimizing feedback control design complexities [3-4]. Studies proved that input shaping technique, is the most effective residual vibration control method for flexible structures [5]. Researchers in [6] proposed an input shaping technique, where reduction in vibration is done by convolving arrangement of the input signals impulses. Recently, several input shaping techniques with some alterations such as unit

magnitude, finite-state, system output speed, output-based, vector diagram approach, negative, two-mode, continuous function and multi-hump extra intensive input shaping techniques [1], have been designed and implemented on various flexible systems such as flexible manipulator as in [7] and non-linear tower crane systems in [8].

Feedback control strategy is capable of payload position tracking as well as oscillation suppression, while input shaping control method is only suitable for oscillation and therefore, several studies have been done on gantry crane payload sway control. Some of the feedback and hybrid control schemes proposed on flexible structures includes Fuzzy – PID based on hybrid optimization as in [9]. In [10], an optimal control of payload sway reduction in gantry crane system was carried out. Optimal controller for under actuated crane system is suggested in [11] while GA optimized hybrid fuzzy control approach was studied in [12]. There is also a robust control method developed in [13] andcrane system vibration control using wave-based robust control in [14]. Optimized PID controller using genetic algorithms (GA) with input shaping technique is proposed in [15] for tracking control and vibration of flexible systems. Optimized command shaper using GA optimization tool in [16] and hybrid output-based control schemes for flexible manipulator in [17] are familiar developments as the PID-type fuzzy logic tuned using PSO in [18].

This paper presents hybrid controllers for sway and precise tracking control of gantry crane system. Hybrid Model dependent and model-free control schemes are proposed and using the simulation studies, the performances of the designed controllers were compared and analyzed.

Next section of the paper presents detail dynamic model of the gantry crane system, hybrid control schemes are given in Section 3. Results and discussion were presented in Section 4. And finally, conclusions and further recommendation was given in Section 5.

2. Gantry Crane System

Gantry crane system is a machine which is used to load and offload goods as well as transport them from one point to another. It is mostly used for heavy machine installations and finds application in nuclear plant, warehouse, seaport and construction industries etc. Fig. 1 shows the picture of gantry crane system. In this work a laboratory scale 2D crane system was used, which consists of trolley and a pendulum as shown in Fig. 2.

The symbols *l, x, θ, m_1* and *m_2*represents the length of the cable, the horizontal position of trolley, the sway angle, the mass of trolley and the payload mass respectively. The system parameters are as in Table 1.

The trolley moves alone the supported and horizontal jib due the applied force *F*, thus move the suspended payload to a point.



Fig. 1. Gantry Crane System.

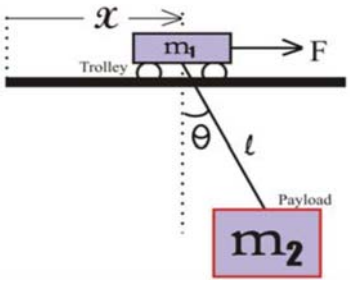


Fig. 2. Schematic diagram of gantry crane system.

Table 1. System parameters.

Parameter	Value /Unit
Mass of payload (m_2)	0.75 kg
Mass of trolley (m_1)	3 kg
Length of the cable (l)	0.75 m
Acceleration due to gravity(g)	9.81 ms^{-2}

2.1. Dynamics Model

In this work, the model of gantry crane system was obtained as in [19], and the dynamics equations are as:

$$F_x = (m_1 + m_2)\ddot{x} + m_2 l(\ddot{\theta}cos\theta - \dot{\theta}^2 sin\theta + 2m_2 \dot{l}\dot{\theta}cos\theta + m_2 \ddot{l}sin\theta), \quad (1)$$

$$l\ddot{\theta} + 2\dot{l}\dot{\theta} + \ddot{x}cos\theta + gsin\theta = 0 \quad (2)$$

Linearizing the Equation (1) and Equation (2) gives

$$F_x = (m_1 + m_2)\ddot{x} + m_2 l\ddot{\theta}, \quad (3)$$

$$l\ddot{\theta} + \ddot{x} + g\theta = 0 \quad (4)$$

Moreover, Equation (3) and Equation (4) can be written in state space as

$$\dot{x} = Ax + Bu \quad (5)$$

and

$$\begin{bmatrix} \dot{x} \\ \ddot{x} \\ \dot{\theta} \\ \ddot{\theta} \end{bmatrix} = \begin{bmatrix} 0 & 1 & 0 & 0 \\ 0 & 0 & \frac{m_2 g}{m_1} & 0 \\ 0 & 0 & 0 & 1 \\ 0 & 0 & -\frac{(m_1+m_2)g}{m_1 l} & 0 \end{bmatrix} \begin{bmatrix} x \\ \dot{x} \\ \theta \\ \dot{\theta} \end{bmatrix} + \begin{bmatrix} 0 \\ \frac{1}{m_1} \\ 0 \\ -\frac{1}{m_1 l} \end{bmatrix} F_x \quad (6)$$

In which x is the trolley position, $\dot{x}$ is the trolley velocity, θ is the sway angle and $\dot{\theta}$ is the angular velocity [19].

3. Controller Design

In this section, Output Based Input Shaping (OBIS) filter was designed using the output of gantry crane system and it was then incorporated into PID, LQR and HODFC separately for sway suppression and trolley position control. Fig. 3, Fig. 4 and Fig. 5 showed the block diagrams of the hybrid control scheme.

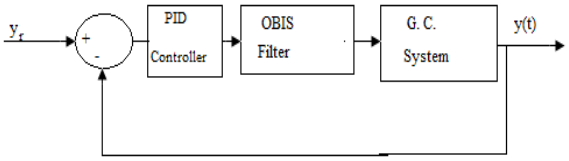


Fig. 3. PID-OBIS Control Block Diagram.

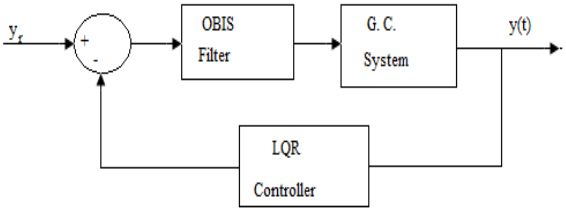


Fig. 4. LQR-OBIS Control Block Diagram.

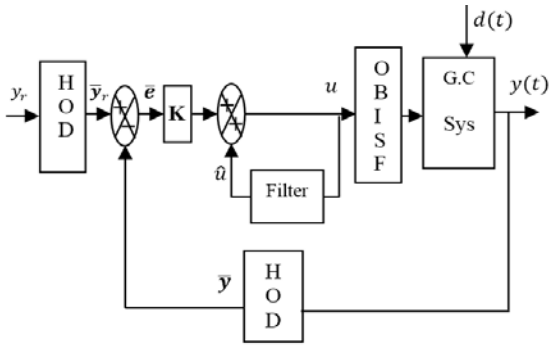


Fig. 5. HODFC-OBIS Control Block Diagram.

3.1. Output Based Input Shaping (OBIS) Filter

In order to design an OBIS filter for GC system, a reference system was designed in [20] as

$$G_r(s) = \left[\frac{\omega_c}{(s+\omega_c)}\right]^n, \quad (7)$$

where n is the order of the system and ω_c is the bandwidth of the system, and is selected based on the time response of the system. The output of the target system $y(t)$ was then decomposed into components as expressed in Equation (8) and Fig. 6.

$$y(t) = \sum_{i=0}^{n} a_i y_i(t), \quad (8)$$

where $y_i(t)$ is the i^{th} component of $y(t)$ and a_i is the coefficient of i^{th} component of $y(t)$.

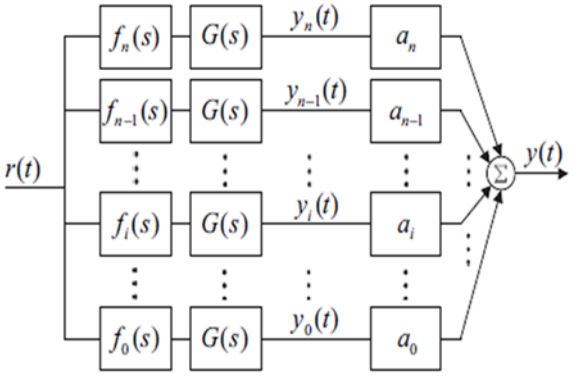


Fig. 6. The decomposition of the system with input shaping filter [20].

In Fig. 6, $G(s)$ is the target system and $f_i(s) = \frac{s^i}{F_d(s)}$ $i = 0, 1, 2..., n$ is the target filter components.

The difference between the unit step response of reference system $y_r(t)$ and that of the target system $y(t)$ was then minimized using a cost function as in Equation (9).

$$E = \int_0^T \omega(t)(y(t) - y_r(t))^2 dt, \quad (9)$$

Putting Equation (8) into Equation (9) yields

$$E(a_1, a_2, ..a_n) = \int_0^T \omega(t)((\sum_{i=0}^{n} a_i y_i(t)) - y_r(t))^2 dt, \quad (10)$$

where $a_1, a_2, \ldots a_n$ are the filter gains and $a_0 = \omega_c^{\,n}$ as in [20]. But this system has double pole at origin hence only $a_1, a_2, \ldots a_n$ are to be obtain.

This system has little or zero vibration, by selecting $a_0 = 3.5^4$, based on time response of this particular system and using Equation (7), the reference system is then given as

$$G_r(s) = \left[\frac{3.5}{(s+3.5)}\right]^4 \quad (11)$$

The filter gains were calculated in MATLAB using the following relation in Equation (12).

$$\begin{bmatrix} a_2 \\ a_4 \end{bmatrix} = \begin{bmatrix} s_{22} & s_{24} \\ s_{42} & s_{44} \end{bmatrix} \begin{bmatrix} s_{2r} \\ s_{4r} \end{bmatrix} \quad (12)$$

Hence, filter gains were obtained as

$a_2 = 564.1179 \quad a_4 = 34.6360$

And the filter equation is obtained as Equation (13).

$$F(s) = \frac{34.6360s^4 + 564.1179s^2}{s^4 + 14s^3 + 73.5s^2 + 171.5s + 150.0625} \quad (13)$$

3.2. LQR Controller

LQR is an optimal state-feedback controller used where the system dynamics are described by a set of *linear differential equations* and the cost is described by a *quadraticfunction.* A control law is selected to regulate the state x and minimizes the performance index as in Equation (14).

$$J = \int_0^\infty (x'Qx + u'Ru)dt \ , \quad (14)$$

where J is the performance index function, *Q* and *R* are weight matrices for the state variable and control variable respectively [21]. And these are semi positive definite matrix and positive definite matrix respectively. The gain vector K can be obtained to satisfy the feedback control law given as

$$u(t) = -Kx(t) \quad (15)$$

The weighting matrices are tuned based on the relative weights given to the system error and control effort. MATLAB program was used in determining the LQR-OBIS hybrid controller gains, *K*.

4. Higher Order Differential Feedback Controller

High order differential feedback control has been successfully applied to linear and nonlinear systems. Differential equation of the nonlinear system with disturbance can be represented as single input single output (SISO) affine system given in Equation (16).

$$y^n = f(x) + b(x)u + d(t), \quad (16)$$

where $u \in \mathcal{R}$ is the control input, $y \in \mathcal{R}$ is the system output, and $\boldsymbol{x} = [x_1, x_2, \dots, x_n] = [y, y^1, y^2, \dots, y^n]^T$ denotes output differential vector, and is also system state vector, y^i denotes the i^{th} differential of $y, f(x)$is an unknownbounded affine function while $d(t)$ is bounded disturbance as studied in [22-24].

The controller design will be divided into three step processes. The first step is to derive an error-based state-space model of the system using the observed states. This observation will be carried out at system's reference input and output respectively, leading to second step of the processes. The second step is to design an appropriate higher-order differentiator (HOD) for the particular problem that will extract the observed states formulated in the first step. Two copies of the HOD system are employed in the controller structure depicted in Fig. 7. The HOD system at the input processes the reference inputy_r to generate the required derivates and extract the observed states. The second HOD system measures the output$y(t)$ in the presence of noise, to generate estimates of the output and its requisite derivatives. Lastly, the third step is to employ, a model-free pole placement procedure with a filter to smoothen and complete the design of the higher-order differential feedback controller (HODFC).

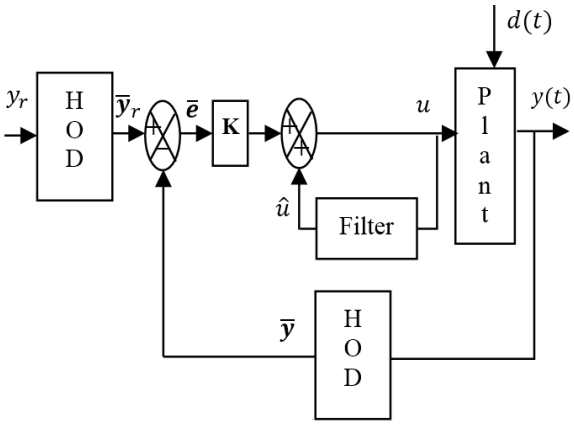


Fig. 7. Higher-order differential feedback controller representation.

Step 1: Derivation of Error, its Derivatives and Observed States

Now, assuming the output of the affine system in Equation (16) is required to track an input trajectory $y_r(t)$ and that all derivatives of both $y_r(t)$ and $y(t)$ are available, then it is possible to derive the error variable and its derivatives as

$$e = y_r - y, \dot{e} = \dot{y}_r - \dot{x}, \dots, e^n = y_r^n - \dot{x}_n \quad (17)$$

Since the error and all its derivatives are available, an error-based state space system can be arranged as

$$\begin{aligned} \dot{e_1} &\equiv e_2, \\ \dot{e_2} &\equiv e_3, \\ \dot{e_n} &\equiv y_r^n - y^n \end{aligned} \tag{18}$$

Hence, one can re-arrange the error vector as

$$\begin{aligned} \boldsymbol{e} = \boldsymbol{y_r} - \boldsymbol{x} &= [e, e_1, e_2, \dots e_n]^T \\ &= [e, e^1, e^2, \dots e^{n-1}]^T \end{aligned} \tag{19}$$

In its extended form it is given as

$$\bar{\boldsymbol{e}} = \bar{\boldsymbol{y}}_r - \bar{\boldsymbol{x}} = [\boldsymbol{e^T}, e^n]^T \tag{20}$$

Considering the system in which the input y_r and the output y are know but $\bar{\boldsymbol{y}}_r$ and $\bar{\boldsymbol{x}}$are unknown. Let us now estimate $\bar{\boldsymbol{y}}_r$ and $\bar{\boldsymbol{x}}$ by observing the states of Equations (21).

$$\begin{aligned} \hat{\bar{\boldsymbol{x}}} &= [\hat{y}, \hat{y}^1, \hat{y}^2, \dots, \hat{y}^n]^T, \\ \hat{\bar{\boldsymbol{y}}}_r &= \left[\hat{y}_r, \hat{y}_r{}^1, \hat{y}_r{}^2, \dots, \hat{y}_r{}^n\right]^T \end{aligned} \tag{21}$$

So that $\hat{y}$ gives an estimate ofy^i. The next step shows how the observed states of the estimating vector x or y_r can be obtained using HOD.

Step 2: Design of Higher Order Differentiator

Given a system of order n, the HOD is an k^{th} order differential system decided for which $k \geq n+1$. The HOD system will then be determined by two model-free parameters k and k_0, with $k_0 \in [2, 50]$ [22, 24]. The parameters are then calculated as

$$K = \frac{k^k}{(k-1)^{k-1}}, \tag{22}$$

$$a_i = k_0^{i-1} K C_{k-1}^{i-1}, \quad i = 1,2, \dots k \tag{23}$$

If the HOD system is to process some measurement$y\,(t)$, the k-system of integrators that implement the HOD is given by Equation (24), [23].

$$\begin{cases} \dot{z}_i = z_{i+1} + a_i(\Upsilon - z1) \\ \dot{z}_k = a_k(\Upsilon - z1) \\ \Upsilon = y(t) + \omega(t) \end{cases} \quad 1 \leq i \leq k-1, \tag{24}$$

where $\Upsilon(t)$ measures the output $y(t)$ with its associated noise $\omega(t)$ and $z_1, \dots, z_k$are states of the system. The estimates of $y(t)$ can then be determined as

$$\begin{cases} \hat{y} = z_1 \\ \hat{y}^i = z_{i+1} + a_i(\Upsilon - z1) \end{cases} \quad i = 1,2, \dots n \tag{25}$$

Given that, $\lim_{t \to 0} \hat{y}^i \equiv y^i$

Step 3: Pole Placement Procedure

The last part of the HODFC controller design is to set Equation (18) to $\boldsymbol{Ke}$ so that

$$y_r^n - y^n = \boldsymbol{Ke} = k_1 e_1 + k_2 e_2 + \cdots k_n e_n \tag{26}$$

And the elements of vector K are chosen so as to make the polynomial $k_1 + k_2 s + k_3 s^2 + \cdots + k_n s^{n-1} + s\hat{}n$ Hurwitz.

The pole placement structure can then be written as

$$u = \boldsymbol{K}e + \hat{u}, \tag{27}$$

where $\hat{u}$ is the filtering signal from the control force u, this can be shown as in [22, 23]

$$\dot{\hat{u}} = -\lambda \hat{u} + u \tag{28}$$

In which; λ is a positive constant.

Hence, the HODFC hybrid controller parameters were selected and optimized using MATLAB/ SIMULINK.

4. Results and Discussion

The Gantry Crane system is simulated to a unit step input to assess the performances of OBIS filter and compares PID-OBIS, LQR-OBIS and HODFC-OBIS hybrid controllers for sway suppression and trolley position tracking. This section presented extensive simulation results and analysis of this algorithms. As shown in Fig. 8 and Fig. 9, significant sway suppression was achieved via OBIS filter.

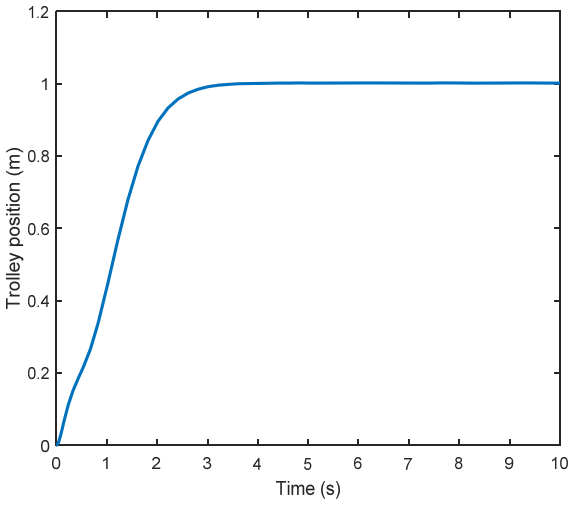


Fig. 8. Trolley Position Travel.

The hybrid control was achieved by incorporating the OBIS filter to each of PID, LQR and HODFC and the optimal gains obtained for these controllers are as PID-OBIS: K_p= 0.74, K_i= 0.97, K_d= 0.13; LQR-

OBIS: K = [0.0003 0.0581 -0.63 -0.03171] and HODFC-OBIS: k=6, k_0=2 and K = [125, 46, 0.3, 0.8, 0.31, 0.51], while the filter was designed as $2/(s+2)$.

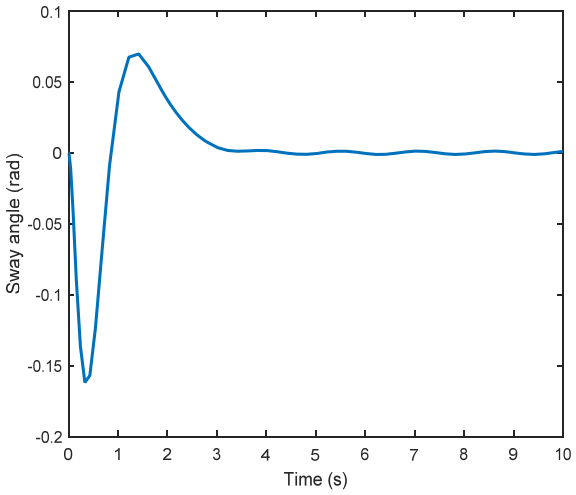


Fig. 9. Angular Sway.

Thus, the simulation results of this controllers for set point trolley position tracking is as shown in Fig. 10, Fig. 11 and Fig. 12. It was observed that a good tracking control was achieved and this was analyzed using time response analysis as in Table 2.

In addition, significant sway reduction was also achieved as shown in Fig. 13, Fig. 14 and Fig. 15. Moreover, Fig. 16 and Fig. 17 compared the tracking and sway reductions control performances of the hybrid controllers. Using mean absolute error and integral absolute error as the performances indexes, the performances of the hybrid controllers for sway reduction was assessed and compared in Table 3. It was observed that LQR-OBIS shows a superior performances, however, HODFC-OBIS been model-free controller is more robust.

Table 2. Time Response Analysis.

Controllers	Max. Overshoot (%)	Settling Time (s)	Rise Time (s)
PID-OBIS	2.4	2.182	1.799
LQR-OBIS	0	2.453	1.936
HODFC-OBIS	0.70	2.440	2.043

Table 3. Performance Indexes.

Controllers	ISE	Sway Reduction (MAE in %)
PID-OBIS	6.24×10^{-6}	82.05
LQR-OBIS	5.23×10^{-6}	85.6
HODFC-OBIS	6.59×10^{-6}	80.26

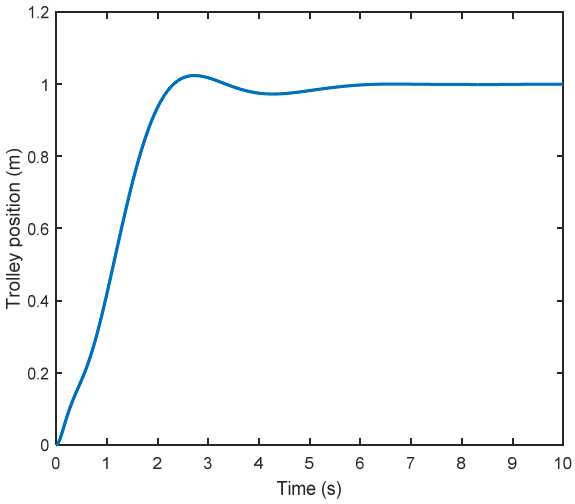


Fig. 10. Trolley Position with PID-OBIS.

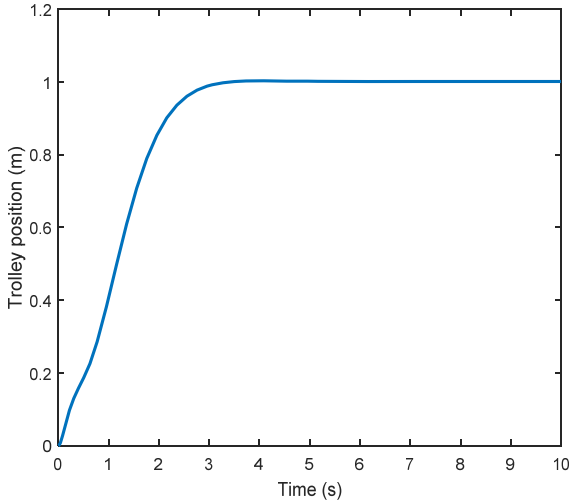


Fig. 11. Trolley Position with LQR-OBIS.

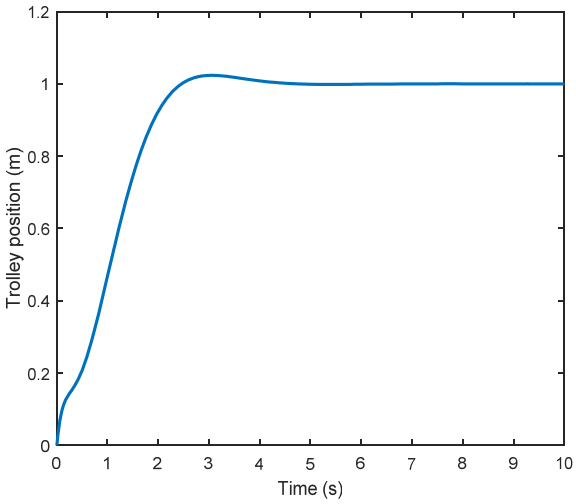


Fig. 12. Trolley Position with HODFC-OBIS.

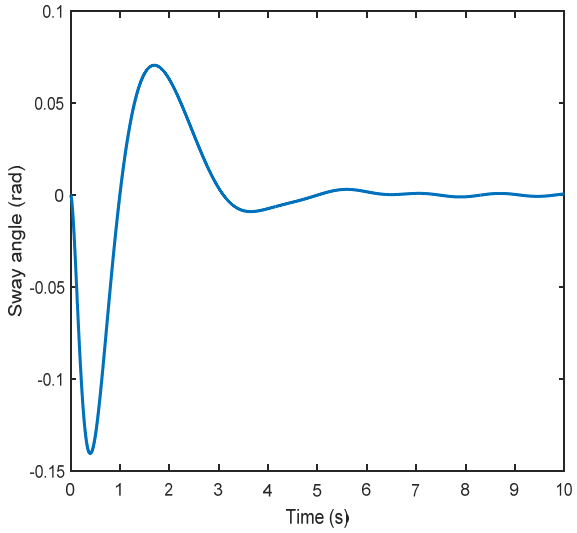


Fig. 13. Sway Angle with PID-OBIS.

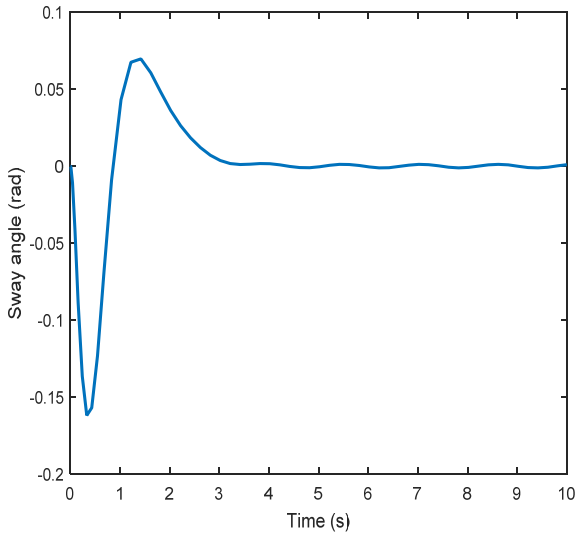


Fig. 14. Sway Angle with LQR-OBIS.

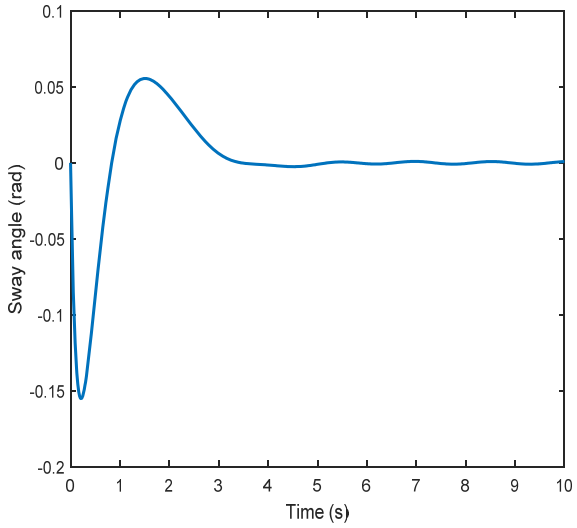


Fig. 15. Sway Angle with HODFC-OBIS.

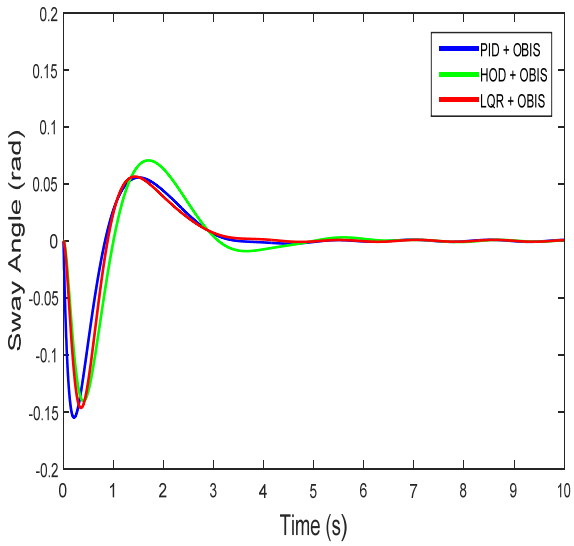


Fig. 16. Sway Angle comparison.

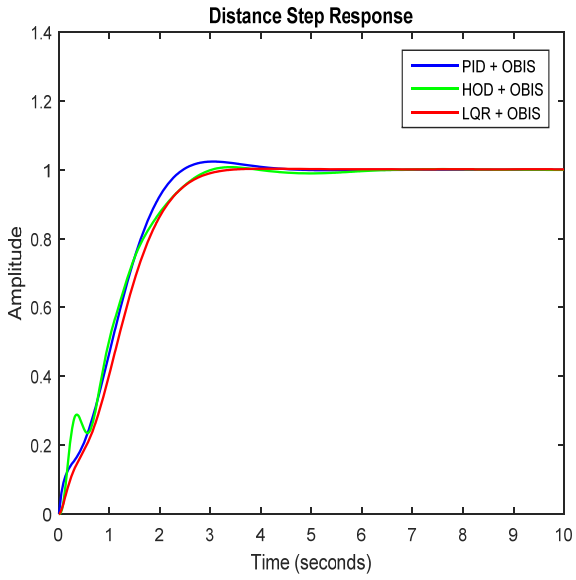


Fig. 17. Trolley Position comparison.

5. Conclusions

In this paper, optimal trolley position tracking and sway suppression control of gantry crane system has been proposed via PID-OBIS, LQR-OBIS and HODFC-OBIS hybrid controllers. The MAE and IAE were used as the performance indexes and a comparative studies using time response analysis was also presented. Simulation study and results analysis show that a good tracking control and sway suppression was achieved. LQR-OBIS controller gave more precise set point tracking but HODFC-OBIS as a model-independent controller, gives an acceptable result in close matching to that of LQR-OBIS in the presence of both internal and external disturbances. An experimental analysis should be conducted to verify this control schemes.

Acknowledgement

The authors gratefully acknowledged the support of Abubakar Tafawa Balewa University (ATBU) Bauchi, Nigeria during the conduct of this study.

References

[1]. N. M. Tahir, K. A. Abubakar, A. U. Sambo, U. I. Bature, N. A Yakub, L. Haliru, Output Based Input Shaping for Sway Control of a 3D Crane System, *International Journal of Electrical and Electronics Engineering*, Vol. 11, Issue 2, 2016, pp. 28-34.

[2]. J. Yoon, S. Nation, W. Singhose, J. E. Vaughan, Control of crane payloads that bounce during hoisting, *IEEE Transactions on Control Systems Technology,* Vol. 22, 2014, pp. 1233-1238.

[3]. N. M. Tahir, A. G. Ibrahim, H. Liman, Hybrid Position and Vibration Control of Nonlinear Crane System, *Journal of Mechanical Engineering and Technology (JMET),* Vol. 9, Issue 2, 2017, pp. 71-86.

[4]. S. Garrido, M. Abderrahim, A. Giménez, R. Diez, C. Balaguer, Anti-swinging input shaping control of an automatic construction crane, *IEEE Transactions on Automation Science and Engineering,* Vol. 5, Issue 3, 2008, pp. 549-557.

[5]. W. Singhose, Command shaping for flexible systems: A review of the first 50 years, *International Journal of Precision Engineering and Manufacturing,* Vol. 10, Issue 4, 2009, pp. 153-168.

[6]. N. C. Singer, W. P. Seering, Preshaping command inputs to reduce system vibration, *Journal of Dynamic Systems, Measurement, and Control,* Vol. 112, Issue 1, 1990, pp. 76-82.

[7]. N. M. Tahir, S. M. Hassan, Z. Mohamed, A. G. Ibrahim, Output Based input Shaping for Optimal Control of Single Link Flexible Manipulator, *International Journal on Smart Sensing & Intelligent Systems,* Vol. 10, Issue 2, 2017, pp. 367-386.

[8]. A. Alhassan, Z. Mohamed, A. M. Abdullahi, A. A. Bature, A. Haruna, N. M. Tahir, Input Shaping Techniques for Sway Control of a Rotary Crane System, *Jurnal Teknologi,* Vol. 80, Issue 1, 2018, pp. 61-69.

[9]. C.-N. Ko, A Fuzzy PID Controller Based on Hybrid Optimization Approach for an Overhead Crane, in *Proceedings of the 14th FIRA RoboWorld Congress*, 2011, pp. 202-209.

[10]. S. Biswas, Optimal control of gantry crane for minimum payload oscillations, in *Proceedings of the International Conference on Dynamic Systems and Applications,* Atlanta, 2003.

[11]. B. Gao, H. Chen, X. Zhang, H. Qi, A practical optimal controller for underactuated gantry crane systems, in *Proceedings of the 1st International Symposium on Systems and Control in Aerospace and Astronautics (ISSCAA'06)*, 2006.

[12]. M. S. Alam, M. O. Tokhi, Hybrid fuzzy logic control with genetic optimisation for a single-link flexible manipulator, *Engineering Applications of Artificial Intelligence*, Vol. 21, Issue 6, 2008, pp. 858-873.

[13]. H. C. Cho, J. W. Lee, Y. J. Lee, K. S. Lee, Lyapunov theory based robust control of complicated nonlinear mechanical systems with uncertainty, *Journal of Mechanical Science and Technology,* Vol. 22, Issue 11, 2008, pp. 2142-2150.

[14]. T. Yang, W. O'Connor, Wave based robust control of a crane system, in *Proceedings of the IEEE International Conference on Intelligent Robots and Systems (RSJ'2006)*, 2006, pp. 2724-2729.

[15]. F. Aldbrez, M. S. Alam, M. O. Tokhi, Input-shaping with GA-tuned PID for target tracking and vibration reduction, in *Proceedings of the IEEE International Symposium on Mediterrean Conference on Control and Automation Intelligent Control,* 2005, pp. 485-490.

[16]. M. Alam, M. Tokhi, Design of a command shaper for vibration control of flexible systems: a genetic algorithm optimisation approach, *Journal of Low Frequency Noise, Vibration and Active Control,* Vol. 26, Issue 4, 2007, pp. 295-310.

[17]. N. M. Tahir, An Output-based Filter for Control of a Single-link Flexible Manipulator, *Universiti Teknologi Malaysia*, 2015.

[18]. S. Bouallègue, J. Haggège, M. Ayadi, M. Benrejeb, PID-type fuzzy logic controller tuning based on particle swarm optimization, *Engineering Applications of Artificial Intelligence,* Vol. 25, Issue 3, 2012, pp. 484-493.

[19]. M. A. Ahmad, Z. Mohamed, Hybrid Fuzzy Logic Control with Input Shaping for Input Tracking and Sway Suppression of a Gantry Crane System, *American Journal of Engineering and Applied Sciences,* Vol. 2, Issue 1, 2009, pp. 241-251.

[20]. J. Han, Z. Zhu, Y. He, J. Qi, A novel input shaping method based on system output, *Journal of Sound and Vibration,* Vol. 335, 2015, pp. 338-349.

[21]. N. M. Tahir, A. A. Bature, U. I. Bature, A. U. Sambo, A. Y. Babawuro, Vibration and Tracking Control of a Single Link Flexible Manipulator Using LQR and Command Shaping, *Journal of Multidisciplinary Engineering Science and Technology*, Vol. 3, 2016, pp. 45-67.

[22]. J. T. Agee, Z. Bingul, S. Kizir, Higher-order differential feedback control of a flexible-joint manipulator, *Journal of Vibration and Control,* Vol. 21, Issue 10, 2015, pp. 1976-1986.

[23]. G. Qi, Z. Chen, Z. Z. Yuan, Model free control of affine chaotic systems, *Physics Letters* A, Vol. 344, Issue 2-4, 2005, pp. 189–202.

[24]. X. Shi, Y. Dai, Z. Liu, G. Qi, High order differential feedback controller and its application in servo control system of machine tools, in *Proceedings of the International Conference on System Science, Engineering and Manufacturing Information*, 2010.

Published by International Frequency Sensor Association (IFSA) Publishing, S. L., 2019 (http://www.sensorsportal.com).